Enhanced thermal conduction by surface phonon-polaritons

Y Wu, Jose Ordonez-Miranda, S Gluchko, R Anufriev, Domingos de Sousa Meneses, Leire del Campo, S Volz, M Nomura

PHYSICS

Enhanced thermal conduction by surface phonon-polaritons

Y. Wu[1]*, J. Ordonez-Miranda[2], S. Gluchko[1,4], R. Anufriev[1], D. De Sousa Meneses[3], L. Del Campo[3], S. Volz[1,4]*, M. Nomura[1]*

Improving heat dissipation in increasingly miniature microelectronic devices is a serious challenge, as the thermal conduction in nanostructures is markedly reduced by increasingly frequent scattering of phonons on the surface. However, the surface could become an additional heat dissipation channel if phonons couple with photons forming hybrid surface quasiparticles called surface phonon-polaritons (SPhPs). Here, we experimentally demonstrate the formation of SPhPs on the surface of SiN nanomembranes and subsequent enhancement of heat conduction. Our measurements show that the in-plane thermal conductivity of membranes thinner than 50 nm doubles up as the temperature rises from 300 to 800 kelvin, while thicker membranes show a monotonic decrease. Our theoretical analysis shows that these thickness and temperature dependencies are fingerprints of SPhP contribution to heat conduction. The demonstrated thermal transport by SPhPs can be useful as a previously unidentified channel of heat dissipation in a variety of fields including microelectronics and silicon photonics.

INTRODUCTION

Phonons are the quasiparticles of lattice vibrations and represent the primary heat carriers in bulk dielectric materials. On the basis of their dispersion relation, phonons are labeled as acoustic or optical. The contribution of optical phonons to the heat conduction is conventionally believed to be negligible because of their low group velocity as compared to that of acoustic phonons (*1*). The thermal conductivity of dielectric membranes is thus typically driven by acoustic phonons and generally reduces with the membrane thickness due to the increasing frequency of surface scattering events (*2*). In the light of the ever-increasing miniaturization of devices with enhanced rates of operation, this reduction in the thermal conductivity causes overheating, low reliability, and reduced lifetime of electronic components (*3*–*6*). Yet, while the thermal transport via acoustic phonons might be at the limit, the heat dissipation might be enhanced via optical phonons coupled with surface electromagnetic waves.

Over the past decade, substantial research efforts have been devoted to the study of these surface waves, because the surface effects predominate over the volumetric ones in nanostructures with high surface-to-volume ratio (*7*). Some types of surface electromagnetic waves may even carry heat (*8*–*11*) and thus improve the thermal performance and stability of nanoscale devices (*12*–*14*). One type of such surface waves is the surface phonon-polaritons (SPhPs), which occurs as a hybrid of optical phonons and surface electromagnetic waves. The SPhPs are essentially evanescent waves that propagate along the surface of polar dielectric membranes (*15*–*18*). SPhPs in the nitrides, especially ultrathin nitrides such as boron nitride, have been exploited for guiding infrared light for optical modulation and photodetection (*19*–*22*). The propagation length of SPhPs is measured in the range of hundreds of micrometers (*23*), which is orders of magnitude longer than the typical mean free path of acoustic phonons. Theoretical models predict that such a long propagation length enables SPhPs to conduct several times more thermal energy than phonons when the membrane thickness is reduced below 100 nm (*15*, *16*). While recent experiments with SiO_2 membranes provided some clues of the SPhP contribution to the heat transport in a limited temperature range (*24*), the reported results are not fully conclusive as the thickness and temperature dependences are hardly different from the corresponding ones in bulk SiO_2, especially due to the presence of the large error bars. For this reason, here, we use a different approach and focus on the temperature evolution in a wide temperature range rather than on thickness dependences. The nature of our experiments thus consists of measurements on the same sample at different temperatures. This allowed us to obtain a decisive evidence of the enhanced thermal conductivity by SPhPs.

RESULTS

Fabrication and measurements

We measure the in-plane thermal conductivity of suspended SiN membranes through the synchronization of an excitation-detection experiment with a micro time-domain thermoreflectance (μTDTR) setup, shown in Fig. 1. Our experiments demonstrate that membranes thinner than 50 nm become more conductive at higher temperatures, as expected for the SPhP contribution, while the thermal conductivity of a 200-nm-thick membrane decreases, in agreement with the phonon counterpart.

To probe the heat conduction in dielectric membranes, we chose amorphous SiN membranes that are commercially available with an excellent quality, high stress, and different thicknesses. After depositing Al transducers on these suspended membranes with thicknesses of 30, 50, 100, and 200 nm, their in-plane thermal conductivity was measured in the range of temperatures from 300 to 800 K by means of the μTDTR technique (Methods). The in-plane thermal conductivity is then extracted from the μTDTR signal by comparing it with an analytical model developed in "Heat diffusion model" section in the Supplementary Materials.

[1]Institute of Industrial Science, The University of Tokyo, Tokyo 153-8505, Japan. [2]Institut Pprime, CNRS, Université de Poitiers, ISAE-ENSMA, F-86962 Futuroscope Chasseneuil, France. [3]CEMHTI, UPR3079, CNRS, Université Orléans, F-45071 Orléans, France. [4]Laboratory for Integrated Micro Mechatronic Systems/National Center for Scientific Research–Institute of Industrial Science (LIMMS/CNRS-IIS), The University of Tokyo, Tokyo 153-8505, Japan.
*Corresponding author. Email: nomura@iis.u-tokyo.ac.jp (M.N.); volz@iis.u-tokyo.ac.jp (S.V.); yunhui@iis.u-tokyo.ac.jp (Y.W.)

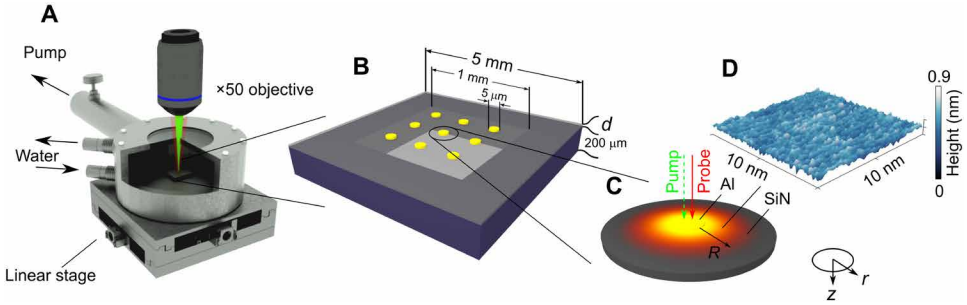

Fig. 1. Scheme of the experimental setup and a SiN membrane with aluminum pads. (**A**) A continuous probe laser beam and a pulsed pump one are focused on the aluminum pad by a (×50) microscope objective. Photo credit: Roman Anufriev, Institute of Industrial Science, The University of Tokyo. (**B**) An image of a suspended SiN membrane supported by a Si frame, which is placed in a vacuum chamber with a temperature-controlled stage. (**C**) The pump laser beam periodically heats up a circular aluminum pad, while the pad reflectance is continuously monitored via the reflected intensity of the probe laser beam impinging into a photodetector. (**D**) An atomic force microscopy (AFM) image of a SiN membrane showing that its surface roughness is smaller than 1 nm.

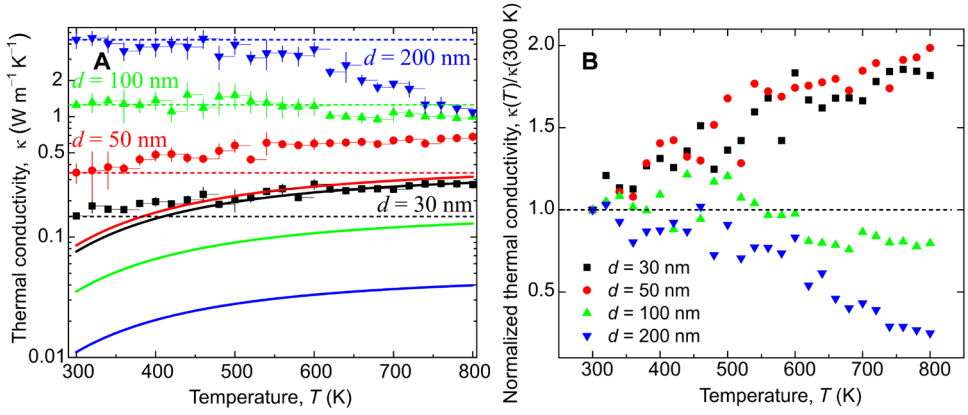

Fig. 2. Temperature dependence of the in-plane thermal conductivity of SiN membranes. Variations of the (**A**) solid symbols represent absolute values of the measured in-plane thermal conductivity of our four SiN samples, and solid lines dedicate their SPhP thermal conductivities predicted by Eq. 1. (**B**) Normalized values of the in-plane thermal conductivity of SiN membranes with four thicknesses. The dashed line is a guide for the eye. Enhancement of heat conduction is observed for 30- and 50-nm-thick membranes at high temperature.

SPhPs enhance thermal conductivity in SiN membranes

Figure 2A reports the measured in-plane thermal conductivity of amorphous SiN membranes of thicknesses 30, 50, 100, and 200 nm in the 300- to 800-K temperature range. The room temperature values of the thermal conductivity are in good agreement with the previous studies (*25*–*27*). The thermal conductivity of the 200-nm-thick membrane at 300 K is 4.36 W $m^{-1}K^{-1}$ and remains nearly temperature independent up to 500 K. Above 500 K, the thermal conductivity decreases according to the power law T^{-2}. This reduction above room temperature is known to be caused by the internal phonon scattering processes, which indicates that heat conduction in this relatively thick membrane are driven by phonons mainly. By contrast, the thermal conductivity of the 100-nm-thick membrane is nearly independent of temperature, with the average values of 1.25 and 0.99 W $m^{-1}K^{-1}$ at 300 and 800 K, respectively. We speculate that this behavior of the thermal conductivity could be due to that the increasing contribution of SPhPs compensates the reduction of the phonon thermal conductivity, as the temperature rises.

As for the two thinner membranes ($d \leq 50$ nm), the increase of the thermal conductivity with temperature becomes notable, so that its value rises from 0.34 W $m^{-1}K^{-1}$ at 300 K to 0.68 W $m^{-1}K^{-1}$ at 800 K for the 50-nm-thick membrane. The thermal conductivity of the 30-nm-thick membrane exhibits a similar enhancement with values of 0.15 and 0.27 W $m^{-1}K^{-1}$ at 300 and 800 K, respectively.

The thermal conductivity trends for the four membranes become even more evident when the values are normalized by the corresponding values at room temperature, as shown in Fig. 2B. The two thinner SiN membranes become twice more conductive as their temperature rises from 300 to 800 K. We also have plotted the measured thermal conductivities of the 30-, 50-, and 100-nm-thick membranes of SiN normalized by the corresponding of the 200-nm-thick membrane (see fig. S6).

DISCUSSION

To better understand the behavior of the measured thermal conductivity, we analyze the SPhP contribution to the heat transport along the surface of SiN membranes. According to the Boltzmann transport equation, under the relaxation time approximation, the SPhP contribution (κ_{SPhP}) to the in-plane thermal conductivity of a membrane of thickness d is given by (*15*)

$$\kappa_{SPhP} = \frac{1}{4\pi d}\int_{\omega_L}^{\omega_H} \hbar\,\omega\Lambda\,\beta_R \frac{\partial f_0}{\partial T} d\omega \quad (1)$$

where $\hbar$ is the reduced Planck constant, $\Lambda = (2\ \mathrm{Im}\ (\beta))^{-1}$ refers to the intrinsic propagation length of SPhPs propagating along the membrane surface with a complex wave vector β, $\beta_R = \mathrm{Re}\ (\beta)$, f_0 represents the Bose-Einstein distribution function; T denotes the average membrane temperature, and ω_H and ω_L stand for the highest and lowest frequencies supporting the propagation of SPhPs, respectively. The effective SPhP propagation should take into account two types of absorption: (i) the intrinsic absorption by the lossy membrane (discussed in "Lossy membrane" section in the Supplementary Materials) and (ii) the absorption or diffraction on the frame of actual sample. The intrinsic propagation length Λ of polaritons propagating along a SiN membrane can be as long as 1 m (see Fig. 3B), while its lateral dimension a (0.5 mm for the 30-nm-thick membrane and 1 mm for the thicker ones) is much smaller. Hence, the SPhP thermal conductivity in Eq. 1 is determined by using the effective propagation length Λ_e given by the Matthiessen's rule $\Lambda_e^{-1}=\Lambda^{-1}+a^{-1}$. This relation establishes that $\Lambda_e \leq a$ and hence allows limiting the propagation distance of polaritons to the real lateral dimension of our samples, as must be.

Equation 1 establishes that the values of κ_{SPhP} are determined by the SPhP dispersion relation $\beta(\omega)$ and by the frequency range of integration, which, for ideal lossless membranes suspended in vacuum ($\varepsilon_1 = 1$), is defined by (*7*) $\mathrm{Re}\ (\varepsilon_2(\omega)) < -1$, with ε_2 being the membrane dielectric function. However, taking into account that lossless materials do not absorb energy and that the heat generated by SPhPs inside a material is proportional to the imaginary part $\mathrm{Im}\ (\varepsilon_2(\omega))$ of its dielectric function (*11*), the SPhP propagating along a lossless membrane does not contribute to the thermal conductivity in Eq. 1. For a lossy material, as is the case of SiN, the dispersion relation of SPhPs along with the condition of their surface confinement establishes that they propagate and contribute to the heat transport in a frequency range much broader than the one supporting their propagation along a lossless material, as was recently demonstrated experimentally (*23*) and is theoretically detailed in "SPhP thermal conductivity modeling" section in the Supplementary Materials. To highlight the advantage of using suspended membrane to demonstrate SPhP contribution (*28*), we analyze the one of SiN membrane on top of an Au nanolayer ("SPhP thermal conductivity of a SiN membrane on top of an Au nanolayer" section in the Supplementary Materials) (*29*).

Taking into account that the SPhP dispersion relation required to calculate the values of κ_{SPhP} is determined by the membrane dielectric function ε_2, which usually depends on temperature (*30*), we measured the dielectric function of our SiN membranes at different temperatures between 300 and 800 K by means of infrared spectroscopy (fig. S2) and is well matched with literature (*31*). The dielectric function of SiN does not substantially change with temperature, as shown in fig. S3; therefore, the temperature evolution of κ_{SPhP} is mainly driven by the temperature derivative of the Bose-Einstein distribution f_0. Figure 3A shows the real (ε_R) and imaginary (ε_I) parts of the dielectric function $\varepsilon_2 = \varepsilon_R + i\varepsilon_I$ measured for the 100-nm-thick membrane at 300 K. The main resonance peaks of ε_I occurs at about 156 Trad s^{-1}, which indicates that the SiN membrane absorbs a notable amount of energy from the electromagnetic field at this frequency. On the other hand, the dip of the real part ε_R at 175 Trad s^{-1} is associated with the maximum confinement of SPhPs to the membrane surface (fig. S4) and therefore provides the main contribution to the SPhP thermal conductivity in Eq. 1. As temperature rises up to 800 K, the representative wavelength range that contributes to SPhP conduction remains from 125 to 225 Trad s^{-1}, which is consistent with the one at room temperature. The spectral thermal conductivity versus frequency is shown in fig. S5.

Figure 3B shows that the SPhP propagation length increases as the membrane thickness decreases, so that its values can be as long as 1 m for a 50-nm-thick membrane. For this reason, we expect a higher thermal conductivity for thinner membranes, as established by Eq. 1. The minimum of the propagation length is not placed at the resonance frequencies of neither the real nor imaginary parts of the dielectric function (see Fig. 2A), because its values are strongly determined by both of these parameters, as detailed in fig. S4. The frequency band gap from 234 to 252 Trad s^{-1} represents the range

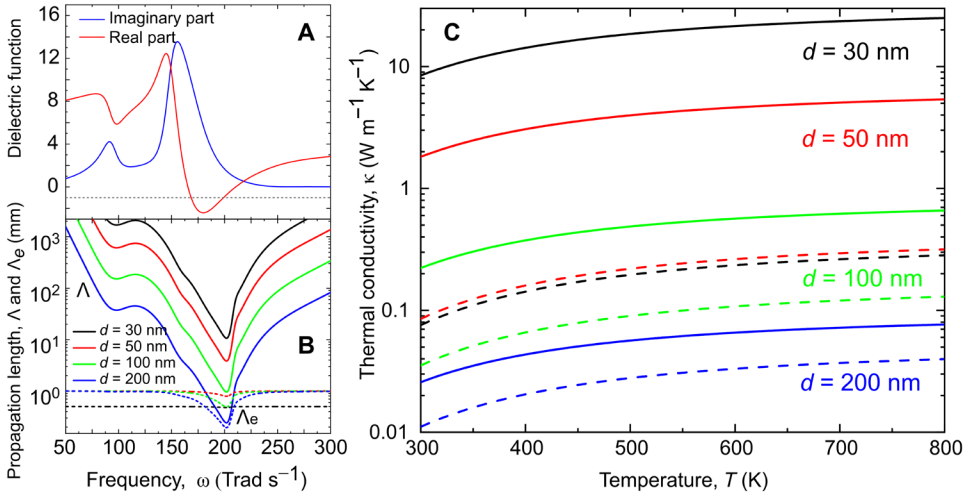

Fig. 3. Theoretical estimation of the SPhP thermal conductivity in SiN membranes. (**A**) Real and imaginary parts of the dielectric function of a 50-nm-thick SiN membrane measured by infrared spectroscopy at 300 K (Methods). (**B**) Propagation length of SPhPs traveling along SiN membranes of different thicknesses without (continuous lines) and with (dashed lines) limited lateral dimension. (**C**) Predicted SPhP thermal conductivity without (continuous lines) and with (dashed lines) limited lateral dimension of SiN membranes at different temperatures.

of frequencies for which the dispersion relation does not have a solution for the SPhP wave vector β, and therefore, the propagation length is not defined.

On the other hand, the SPhP thermal conductivity increases for thinner and/or hotter membranes, as shown in Fig. 3C. This behavior is the opposite to the one exhibited by the phonon thermal conductivity of typical dielectrics and thus represents the fingerprints of the SPhP contribution to heat transport along membranes. With analytical model similar to the one we used above, some studies predict the enhancement in thermal conductivity due to SPhPs in thinner SiO_2 and SiC membranes (*15*, *16*).

Note that for the thinnest film (d = 30 nm), the values of the measured thermal conductivity $\kappa_{exp} = \kappa_{SPhP} + \kappa_{phonon}$ are in good agreement with their SPhP counterparts (κ_{SPhP}), for temperatures higher than 500 K, where the phonon contribution (κ_{phonon}) is expected to be relatively small. For lower temperatures, on the other hand, the latter contribution does matter and hence $\kappa_{exp} > \kappa_{SPhP}$. Furthermore, the predicted SPhP thermal conductivity κ_{SPhP} for the 30-nm-thick membrane is lower than the one for a 50-nm-thick membrane due to its relatively small lateral dimension and hence effective propagation length, as shown in Fig. 3B. The three thicker membranes (d = 50, 100, and 200 nm) have the same lateral dimension a = 1 mm, and therefore, their polariton thermal conductivities reduce as their thicknesses increase. On the other hand, given that the phonon thermal conductivity of a SiN membrane increases with its thickness, the measured thermal conductivity κ_{exp} of the three thicker membranes is expected to be determined by the phonon contribution mainly, which explains the remarkable difference between κ_{exp} and κ_{SPhP} for these latter membranes.

In amorphous material, phonons are catalogued as propagons, diffusons, and locons based on the vibrational modes (*32*). Propagons and diffusons carry most of the heat in bulk amorphous materials, whereas the flux contribution of locons remains negligible. The temperature dependence of propagons might be discarded due to the predominance of surface scattering. Although the diffuson thermal conductivity also increases with temperature (*33*), its contribution is enhanced by only about 6% from 300 to 800 K, as detailed in "Diffuson thermal conductivity in amorphous SiN." section in the Supplementary Materials. This weak enhancement is thus negligible in comparison with the 100% increase observed on the measured thermal conductivity of the 30-nm-thin film, which confirms that this latter sizable increase can only be attributed to SPhPs, as predicted by theory. Thus, we attribute the thermal conductivity increase predominantly by the contribution of SPhPs.

In conclusion, we experimentally measured the in-plane thermal conductivity of amorphous SiN membranes at different temperatures. A notable increase of the thermal conductivity with temperature in the 300 - 800 K range has been observed for membranes thinner than 100 nm. We attribute this enhancement to the propagation of SPhPs along the membrane interfaces. Our results demonstrate that the reduction of the phonon thermal conductivity of nanomaterials can be compensated for by the increase of its counterpart driven by the propagation of SPhPs and even double the thermal energy transport. Thus, this work uncovers a new channel of heat transport along polar dielectrics and lays the foundations for improving the heat dissipation in microelectronics and efficiency in silicon photonics.

METHODS

Sample preparation

Samples of amorphous SiN membranes with thicknesses of 30, 50, 100, and 200 nm are suspended in 1.0 × 1.0 – mm^2 rectangular windows of Si. These commercial high-stress (≈250 MPa) membranes were flat (curvature radius of 4 m) and did not exhibit wrinkles. A circular aluminum pad of 5 μm in diameter and 70 nm in height was deposited on top of each membrane through electron beam lithography and electron beam–assisted physical deposition (Ulvac EX-300). The separation distance between these metallic pads was chosen long enough (>200 μm) to minimize their contribution to the total thermal properties of the SiN membranes. The spatial distribution of the aluminum pads is shown in the optical microscopy image (fig. S1). Furthermore, on the basis of atomic force microscopy (AFM) images of the SiN membranes, their surface roughness was estimated to be smaller than 1 nm (Fig. 1D). This roughness is negligible compared to the SPhP wavelength ($2\pi/\beta_R$), and therefore, it should not attenuate the propagation of SPhPs along the SiN membrane interfaces.

Experimental setup

To probe the heat transport in our SiN membranes at different temperatures, we placed them in a vacuum chamber with a temperature-controlled stage for performing measurements above room temperature (300 to 800 K). The convection effects were cancelled out with a chamber pressure below 10^{-3} Pa.

The thermal conductivity of the membranes was measured by means of the μTDTR method shown in Fig. 1. The working principle of this all-optical pump-probe technique consists in focusing a continues-wave "probe" laser beam (785 nm) and a pulsed "pump" (642 nm) one on the aluminum pad by means of a (×50) microscope objective. The pump beam is used to periodically heat up the aluminum pad, which changes its reflectance that is continuously measured by monitoring the intensity of the reflected probe beam through a photodetector connected to a digital oscilloscope. Given that the reflectance of a material is proportional to its temperature via the thermoreflectance coefficient, each pulse of the pump beam generates a jump in the signal of the reflected probe beam. As heat gradually spreads from the aluminum pad through the underlying membrane, the temperature and thus the pad reflectance return to the initial values. The probe beam records this process as a gradual return of the reflected laser intensity. During one iteration, the μTDTR system integrates the data from the lock-in detector for 10^4 pump pulses. To further reduce the noise, we accumulate the signal for 1 min, which consists of 10^3 of such iterations. More details of our experimental setup can be found in the literature (*34*). Last, the measured temporal variations of temperature are combined with an analytical model ("Heat diffusion model" section in the Supplementary Materials) to extract the in-plane thermal conductivity of our SiN membranes.

SUPPLEMENTARY MATERIALS

Supplementary material for this article is available at http://advances.sciencemag.org/cgi/content/full/6/40/eabb4461/DC1

REFERENCES AND NOTES

1. Y. Zhang, Y. Wang, The effect of coherent optical phonon on thermal transport. *Appl. Phys. A* **117**, 2183–2188 (2014).
2. P. Nath, K. L. Chopra, Thermal conductivity of amorphous vs crystalline Ge and GeTe films. *Jpn. J. Appl. Phys.* **13**, 781 (1974).

3. S. Volz, J. Shiomi, M. Nomura, K. Miyazaki, Heat conduction in nanostructured materials. *J. Therm. Sci. Technol.* **11**, JTST0001 (2016).
4. S. Volz, J. Ordonez-Miranda, A. Shchepetov, M. Prunnila, J. Ahopelto, T. Pezeril, G. Vaudel, V. Gusev, P. Ruello, E. M. Weig, M. Schubert, M. Hettich, M. Grossman, T. Dekorsy, F. Alzina, B. Graczykowski, E. Chavez-Angel, J. S. Reparaz, M. R. Wagner, C. M. Sotomayor-Torres, S. Xiong, S. Neogi, D. Donadio, Nanophononics: State of the art and perspectives. *Eur. Phys. J. B* **89**, 15 (2016).
5. D. G. Cahill, W. K. Ford, K. E. Goodson, G. D. Mahan, A. Majumdar, H. J. Maris, R. Merlin, S. R. Phillpot, Nanoscale thermal transport. *J. Appl. Phys.* **93**, 793–818 (2003).
6. M. Nomura, J. Shiomi, T. Shiga, R. Anufriev, Thermal phonon engineering by tailored nanostructures. *Jpn. J. Appl. Phys.* **57**, 080101 (2018).
7. F. Yang, J. R. Sambles, G. W. Bradberry, Long-range surface modes supported by thin films. *Phys. Rev. B* **44**, 5855–5872 (1991).
8. K. Joulain, J.-P. Mulet, F. Marquier, R. Carminati, J.-J. Greffet, Surface electromagnetic waves thermally excited: Radiative heat transfer, coherence properties and Casimir forces revisited in the near field. *Surf. Sci. Rep.* **57**, 59–112 (2005).
9. D.-Z. A. Chen, G. Chen, Measurement of silicon dioxide surface phonon-polariton propagation length by attenuated total reflection. *Appl. Phys. Lett.* **91**, 121906 (2007).
10. D.-Z. A. Chen, G. Chen, Heat flow in thin films via surface phonon-polaritons. *Front. Heat Mass Transf.* **1**, 023005 (2010).
11. G. Baffou, C. Girard, R. Quidant, Mapping heat origin in plasmonic structures. *Phys. Rev. Lett.* **104**, 136805 (2010).
12. J.-P. Mulet, K. Joulain, R. Carminati, J.-J. Greffet, Nanoscale radiative heat transfer between a small particle and a plane surface. *Appl. Phys. Lett.* **78**, 2931–2933 (2001).
13. V. Dusastre, L. Martiradonna, Materials for sustainable energy. *Nat. Mater.* **16**, 15 (2017).
14. K. Biswas, J. He, I. D. Blum, C.-I. Wu, T. P. Hogan, D. N. Seidman, V. P. Dravid, M. G. Kanatzidis, High-performance bulk thermoelectrics with all-scale hierarchical architectures. *Nature* **489**, 414–418 (2012).
15. D.-Z. A. Chen, A. Narayanaswamy, G. Chen, Surface phonon-polariton mediated thermal conductivity enhancement of amorphous thin films. *Phys. Rev. B* **72**, 155435 (2005).
16. J. Ordonez-Miranda, L. Tranchant, T. Tokunaga, B. Kim, B. Palpant, Y. Chalopin, T. Antoni, S. Volz, Anomalous thermal conductivity by surface phonon-polaritons of polar nano thin films due to their asymmetric surrounding media. *J. Appl. Phys.* **113**, 084311 (2013).
17. J.-J. Greffet, R. Carminati, K. Joulain, J.-P. Mulet, S. Mainguy, Y. Chen, Coherent emission of light by thermal sources. *Nature* **416**, 61–64 (2002).
18. M. Francoeur, M. P. Mengüç, R. Vaillon, Local density of electromagnetic states within a nanometric gap formed between two thin films supporting surface phonon polaritons. *J. Appl. Phys.* **107**, 034313 (2010).
19. A. Didari, E. B. Elçioğlu, T. Okutucu-Özyurt, M. P. Mengüç, Near-field radiative transfer in spectrally tunable double-layer phonon-polaritonic metamaterials. *J. Quant. Spectrosc. Rad. Transfer* **212**, 120–127 (2018).
20. B. Zhao, Z. M. Zhang, Enhanced photon tunneling by surface plasmon–phonon polaritons in Graphene/hBN heterostructures. *J. Heat Transfer* **139**, 022701 (2017).
21. Q. Zhang, Z. Zhen, Y. Yang, G. Gan, D. Jariwala, X. Cui, Hybrid phonon-polaritons at atomically-thin van der Waals heterointerfaces for infrared optical modulation. *Opt. Express* **27**, 18585–18600 (2019).
22. A. Y. Nikitin, E. Yoxall, M. Schnell, S. Vélez, I. Dolado, P. Alonso-Gonzalez, F. Casanova, L. E. Hueso, R. Hillenbrand, Nanofocusing of hyperbolic phonon polaritons in a tapered boron nitride slab. *ACS Photonics* **3**, 924–929 (2016).
23. S. Gluchko, B. Palpant, S. Volz, R. Braive, T. Antoni, Thermal excitation of broadband and long-range surface waves on SiO_2 submicron films. *Appl. Phys. Lett.* **110**, 263108 (2017).
24. L. Tranchant, S. Hamamura, J. Ordonez-Miranda, T. Yabuki, A. Vega-Flick, F. Cervantes-Alvarez, J. J. Alvarado-Gil, S. Volz, K. Miyazaki, Two-dimensional phonon polariton heat transport. *Nano Lett.* **19**, 6924–6930 (2019).
25. A. J. Griffin, F. R. Brotzen, P. J. Loos, The effective transverse thermal conductivity of amorphous Si_3N_4 thin films. *J. Appl. Phys.* **76**, 4007–4011 (1994).
26. C. H. Mastrangelo, Y.-C. Tai, R. S. Muller, Thermophysical properties of low-residual stress, Silicon-rich, LPCVD silicon nitride films. *Sensor. Actuat. A Phys.* **23**, 856–860 (1990).
27. S.-M. Lee, D. G. Cahill, Heat transport in thin dielectric films. *J. Appl. Phys.* **81**, 2590–2595 (1997).
28. J. Ordonez-Miranda, L. Tranchant, Y. Chalopin, T. Antoni, S. Volz, Thermal conductivity of nano-layered systems due to surface phonon-polaritons. *J. Appl. Phys.* **115**, 054311 (2014).
29. M. A. Ordal, L. L. Long, R. J. Bell, S. E. Bell, R. R. Bell, R. W. Alexander Jr., C. A. Ward, Optical properties of the metals Al, Co, Cu, Au, Fe, Pb, Ni, Pd, Pt, Ag, Ti, and W in the infrared and far infrared. *Appl. Opt.* **22**, 1099–1120 (1983).
30. K. Joulain, Y. Ezzahri, J. Drevillon, B. Rousseau, D. D. S. Meneses, Radiative thermal rectification between SiC and SiO_2. *Opt. Express* **23**, A1388–A1397 (2015).
31. G. Cataldo, J. A. Beall, H.-M. Cho, B. M. Andrew, M. D. Niemack, E. J. Wollack, Infrared dielectric properties of low-stress silicon nitride. *Opt. Lett.* **37**, 4200–4202 (2012).
32. P. B. Allen, J. L. Feldman, Thermal conductivity of disordered harmonic solids. *Phys. Rev. B* **48**, 12581–12588 (1993).
33. Y. Liao, J. Shiomi, Akhiezer Mechanism Dominates Relaxation of Propagons in Amorphous at Room Temperature. arXiv:2006.07773 (2020).
34. R. Anufriev, S. Gluchko, S. Volz, M. Nomura, Quasi-ballistic heat conduction due to Lévy phonon flights in silicon nanowires. *ACS Nano* **12**, 11928–11935 (2018).

Acknowledgments: We thank Y. Liao and J. Shiomi for the discussions on diffuson thermal conductivity in amorphous SiN. **Funding:** This work was supported by the CREST JST grant numbers JPMJCR19Q3 and JPMJCR19I1 and KAKENHI grant numbers 15H05869 and 17H02729. **Author contributions:** Y.W., M.N., and S.V. designed the experiment. S.G. and R.A. fabricated the samples. R.A. performed the AFM characterization. Y.W. performed the μTDTR measurements and wrote the paper. J.O.-M. developed the theoretical and analytical models. J.O.-M. and R.A. contributed to writing the paper. D.D.S.M. and L.D.C. performed the infrared spectroscopy measurement. S.V. and M.N. contributed to the interpretation of the results and supervised the entirety of the work. All authors contributed to the analysis and discussion of the results. **Competing interests:** The authors declare that they have no competing interests. **Data and materials availability:** All data needed to evaluate the conclusions in the paper are present in the paper and/or the Supplementary Materials. Additional data related to this paper may be requested from the corresponding authors.

Submitted 25 February 2020
Accepted 4 August 2020
Published 30 September 2020
10.1126/sciadv.abb4461

Citation: Y. Wu, J. Ordonez-Miranda, S. Gluchko, R. Anufriev, D. D. S. Meneses, L. Del Campo, S. Volz, M. Nomura, Enhanced thermal conduction by surface phonon-polaritons. *Sci. Adv.* **6**, eabb4461 (2020).

Enhanced thermal conduction by surface phonon-polaritons

Y. Wu, J. Ordonez-Miranda, S. Gluchko, R. Anufriev, D. De Sousa Meneses, L. Del Campo, S. Volz and M. Nomura

Sci Adv **6** (40), eabb4461.
DOI: 10.1126/sciadv.abb4461